Chia-Ming Lo[(1)], Lun-Wei Wei[(1)], Cheng-Yang Hsiao[(1)], Yen-Hsiang Lin[(1)], Chin-Tung Cheng[(1)], Ming-Lang Lin[(2)]

A Kinematic Model of the Hsiaolin Landslide Calibrated to the Landslide Deposition pattern

(1) Geotechnical Engineering Research Center, Sinotech Engineering Consultants, INC.
(2) Department of Civil Engineering, National Taiwan University

Abstract This paper presents results of a case study on the Hsiaolin catastrophic landslide, including its kinematic process and the geometry of deposition. Based on geomorphologic analysis, the landslide initiated in thick, multi-aged colluvium soils at the headwaters of a small stream upslope of Hsiaolin village. A 3D discrete element program, PFC3D was used to model the kinematic process that led to the landslide and destruction of Hsiaolin village. The landslide advanced from debris slide to debris avalanche during the kinematic process. Assuming a friction coefficient of each particle of 0.1, the predicted maximum velocity was about 70 m/sec, a velocity which permits the debris to cross Qishanxi stream and deposit on the opposite bank. Based on simulation results, Hsiaolin village was inundated in 60 to 65 seconds after failure initiation; at 112 seconds after the event, the debris avalanche came to rest, forming a landslide dam. This study demonstrates that the discrete element method, which is not a main stream computational tool, has great potential for gaining mechanical understanding, and also for hazard delineation.

Keywords Catastrophic landslide, kinematic process, geomorphologic analysis, Numerical modeling

Introduction

On August 9 2009, typhoon Morakot made landfall in southern Taiwan. The accompanying torrential rain was exceptionally heavy, and triggered a catastrophic landslide that both swept and buried the entire Hsiaolin, a village in Jiaxian township, Kaohsiung County, Taiwan (Fig.1). The main bulk of the landslide occurred at approximately 6:00 AM and initiated from a slope about 800 m to 1200 m above the riverbed. A huge amount of fragmented rock material moved quickly downward and became a debris avalanche. Part of the debris rushed over a High-Level Terrace, spread along the hillslope, and finally reached and destroyed the entire Hsiaolin village.

The mechanism behind the Hsiaolin landslide was subject of intensive research and study. The collapse area of the Hsiaolin landslide was initially covered by thick colluvium from a number of past events prior to the Morakot onslaught. This colluvium provided materials to construct landslide dam and buried Hsiaolin village. Slope deformation history and landslide kinematic process hence are the keys to the cause of Hsiaolin village destruction. Moreover, large, high-velocity landslides, especially the disintegrative rockslides that develop into debris avalanches are remarkable geological phenomena (Steven and Simon, 2006). Velocity is the most important parameter determining the destructive potential of these landslides. "Catastrophic" velocities of the order of several meters per second are attained only by landslide avalanches (Hungr, 2007). However, there has thus far been relatively little research into the landslide kinematic process. In an effort to understand the kinematic of the Hsiaolin catastrophic landslide and to provide reference in planning of mitigation strategies for the same area, geomorphologic analyses and numerical simulations were carried out.

Terrain and Geology of the Hsiaolin Landslide

In a west to east order, the study area can be topographically described as being comprised of the Qishanxi stream (EL. 365 m), the beach strand, Hsiaolin village, High-Level Terrace, 590 Height, and Xiandushan (EL. 1,445 m). In a south to north order, the main streams in the study area are Jiaopuxi, Unnamed Creek A, and Unnamed Creek B. The difference in elevation is 1,000 m from Xiandushan to the Qishanxi stream, sufficient to induce high velocity run and enlarge the extent of the landslide.

Geologic strata exposed at Xiandushan comprise the Yenshuikeng Shale (Sung et al., 2000) in the upper half of the section and the Tangenshan Formation (Sung et al., 2000) in the lower (Fig.2). The north cliff of Xiandushan at the right bank of Unnamed Creek A is a cataclinal slope, whereas the south cliff at the left bank of Unnamed Creek A is an anaclinal slope. Topographically speaking, Xiandushan terrain belongs to the narrow ravine towards the Qishanxi stream, and appeared to be composed of old landslide deposits with retrogressive erosion. Geologically speaking, there are unfavorable wedges formed by combinations of bedding planes at north side and joints or small fault at south side; and all these wedges occur in an adverse overhanging configuration. The source area of the Hsiaolin landslide was covered by a very thick bed of colluvium attributable to various past events. These colluvial materials afforded a condition for water

infiltration that readily saturated the unstable slope. (Lee et al, 2009).

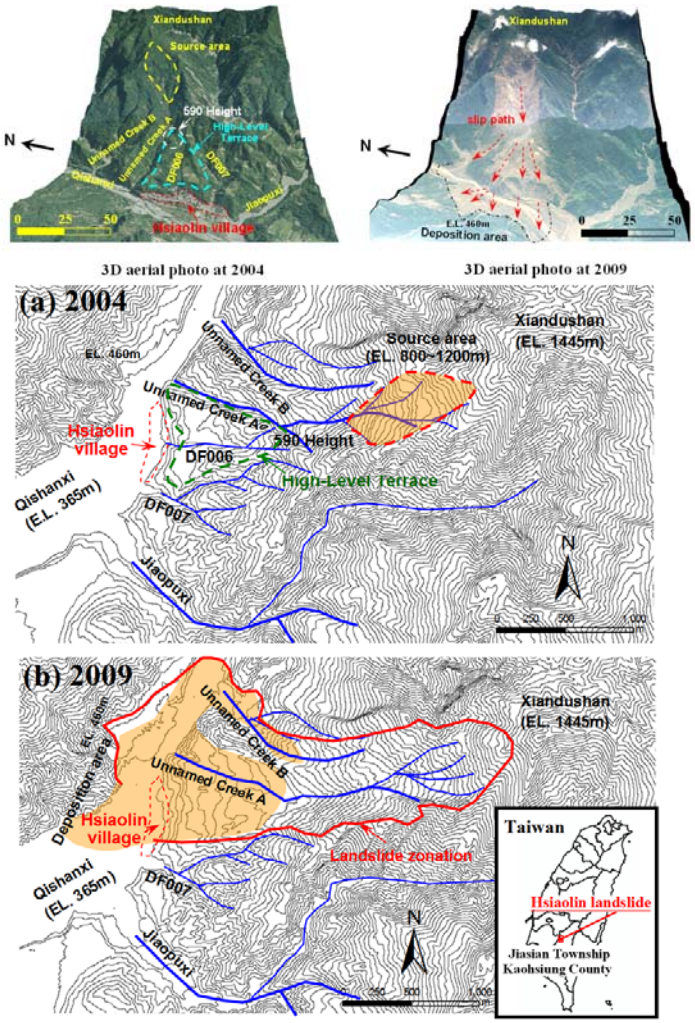

Figure 1 Topographic maps and aerial photos of the study area.

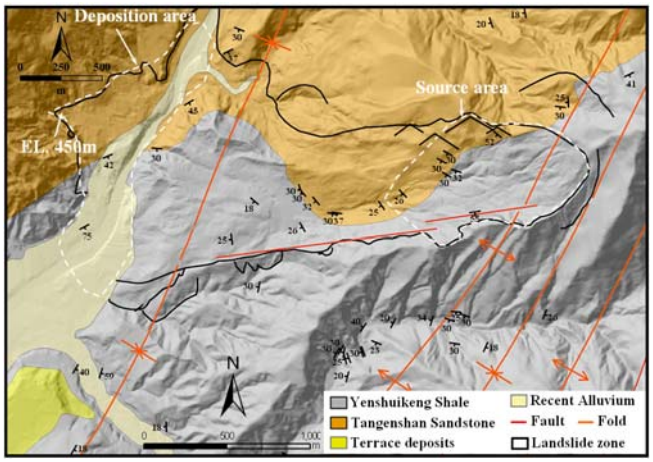

Figure 2 The geologic maps of the study area (Lee et al., 2009).

Geomorphologic Features of the Hsiaolin Landslide

Under geomorphologic analysis (Fig.3), 1904 topographic map presents a dendritic drainage pattern on the upstream of Unnamed Creek A. In 1936, the upstream gully of the right bank was not present; parts of the colluvium deposits were present on the gully and formed a hummocky surface. Moreover, the colluvium of various events constructed the hummocky terrain within the top of High-Level Terrace and deflected the river course of Unnamed Creek A. In 1996, most of the hummocky surface on the upstream, and 590 Height still existed. 590 Height finally collapsed under attack from the Hsiaolin catastrophic landslide, and the hummocky terrain was eradicated and transformed into the smooth terrain, as verified in 2009. In the same year, parts of the colluvium were still deposited on the upstream of Unnamed Creek A; most of the debris, however were deposited on High-Level Terrace and at the Qishanxi stream.

A number of points are worthy of note here. First, most of the hummocky terrain on the source area is the result of burying upstream gullies during 1936-2009. This is indicative of gravitational slope deformation processes and convincing evidence of landslide deposition on the source area. Second, 590 Height was formed by deposition of colluvial materials, and consequently deflected the river course. These results were used to reconstruct the pre-collapse area. Third, huge amount of slide materials and high-level potential energy combined were sufficient to generate tremendous dynamic energy that was high enough to cause collapse of 590 Height, and to trigger a debris avalanche that overflowed High-Level Terrace.

Based on topographic analysis using a 5 m resolution DEM (Fig.4), the Hsiaolin landslide was shown to be about 3 km long, 1-1.5 km wide, about 650 m drop height, with a total area of about 109 ha, and a total volume of about 25 million cubic meters. Most debris reached the Qishanxi stream and constructed the landslide dam. According to the mapping results (Dong et al., 2011), the highest and the lowest elevations of the landslide dam were 475 m and 420 m, respectively, with a mean height of 70 m. The cross-river length and the along-river width of the dam were are 450 m and 750 m, respectively.

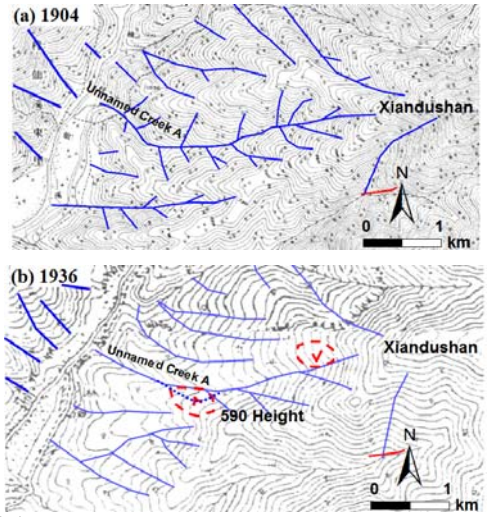

Figure 3(A) The development process of hummocky terrain with river course of Unnamed Creek A in 1904 and 1936.

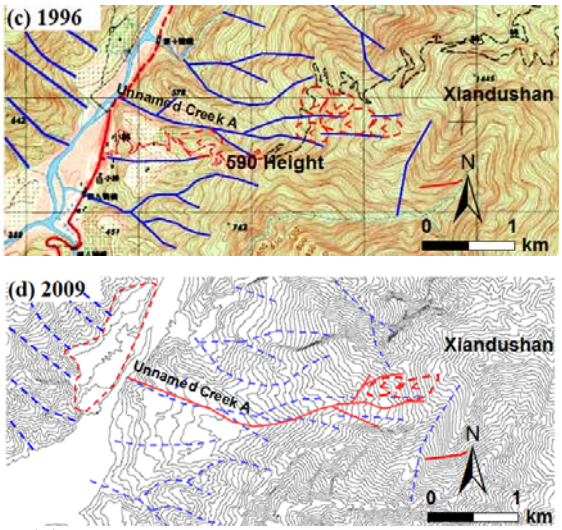

Figure 3(B) The development process of hummocky terrain with river course of Unnamed Creek A in 1996 and 2009.

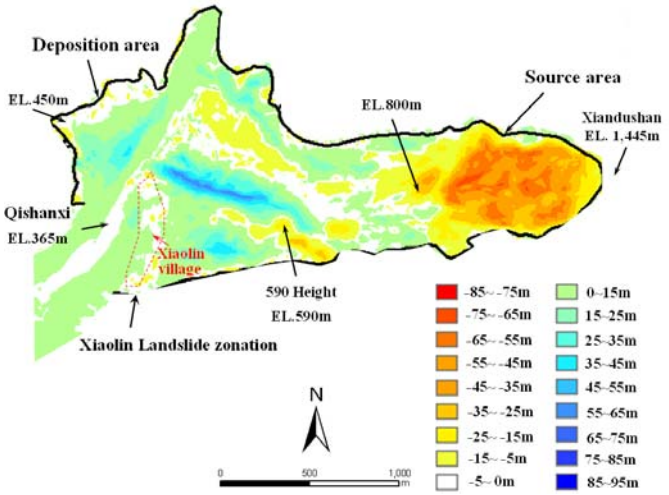

Figure 4 The result of DEM subtraction by 5m resolution between 2004 and 2009.

Numerical modeling of the Hsiaolin landslide

PFC (Particle Flow Code) was implemented through the development of the Discrete Element Method proposed by Cundall and Strack (1979). The elements of PFC model mainly include particles and walls, the sliding surface of the collapse area in the Hsiaolin landslide model was constructed by 13,456 wall elements based on a 40×40 m DEM made after Morakot event, and the deposit area was based on a 40×40 m DEM made before the Morakot event (Fig.5), the total length was 4300 m, the total width was 2300 m. The sliding mass was constructed uses 27,000 balls with radius of 5-6 meters, 25,000 balls were placed on source and 2,000 balls on 590 Height (Fig.5).

To use PFC models as reliable simulation tools, it is necessary to establish reasonable relations between the numerical parameters and the mechanical characteristics of real problems (Potyondy and Cundall, 2004). In discrete element methods, the macroscopic behavior of the granular media depends on the contact mechanical properties, and there is no straightforward solution relating these parameters. Thus we performed a series of compression numerical tests on granular samples to derive the rock mechanical macro-properties of the granular assembly (Fig.6). The 3D granular sample consists of 8574 balls. The numerical parameters obtained for test are the Young's modulus E=4.8 GPa, the Poisson's ratio υ=0.14, and the compression strength UCS=16 MPa. The macroscopic properties of the numerical sample are similar to the properties of the rock samples from the Yenshuikeng Shale, as determined from laboratory tests (Tab.1). Tab.2 is the numerical parameters of PFC modeling.

Table 1 The comparison results of uniaxial compression test and Yenshuikeng Shale test.

Item	Yenshuikeng Shale	PFC Model (Marco-properties)
Density	2,600 kg/m^3	2,600 kg/m^3
Young's Modulus (Ec)	4.8 GPa	4.76 GPa
UCS	15.8 MPa	16.0 MPa

Table 2 The numerical parameters of PFC modeling.

	The numerical parameters of compression test	The numerical parameters of the landslide
Simulation Volume (m^3)	2.67×10^{-3}	2.47×10^{7}
Number of wall elements	2	13,456
Number of particles	28,250	27,000
Particle density (kg/m^3)	2,600	2,600
Range of particle radius (m)	0.0025-0.003	5-6
Normal stiffness (KN/m)	5×10^{7}-6×10^{7}	9.5×10^{10}-1×10^{11}
Shear stiffness (KN/m)	2.5×10^{7}-3×10^{7}	4.8×10^{10}-5×10^{10}
Friction coefficient of ball	0.6	0.05-0.2
Friction coefficient of wall	0.6	0.6
Normal stiffness of parallel bonds (KN/m^3)	8×10^{11}-9.5×10^{11}	4×10^{8}-4.8×10^{8}
Shear stiffness of parallel bonds (KN/m^3)	4×10^{11}-4.8×10^{11}	2×10^{8}-2.4×10^{8}
Normal strength of parallel bonds (Mpa)	16	16
Shear strength of parallel bonds (MPa)	8	8
Critical damping ratio (Normal)	0.4	0.4
Critical damping ratio (Shear)	0.2	0.2

Table 3 The damping coefficient parameters of PFC modeling.

Slope Materials	Damping coefficient
Bedrock	0.21
Bedrock covered by large blocks	0.32
Debris formed by uniform distributed elements	0.36
Soil covered vegetation	0.40

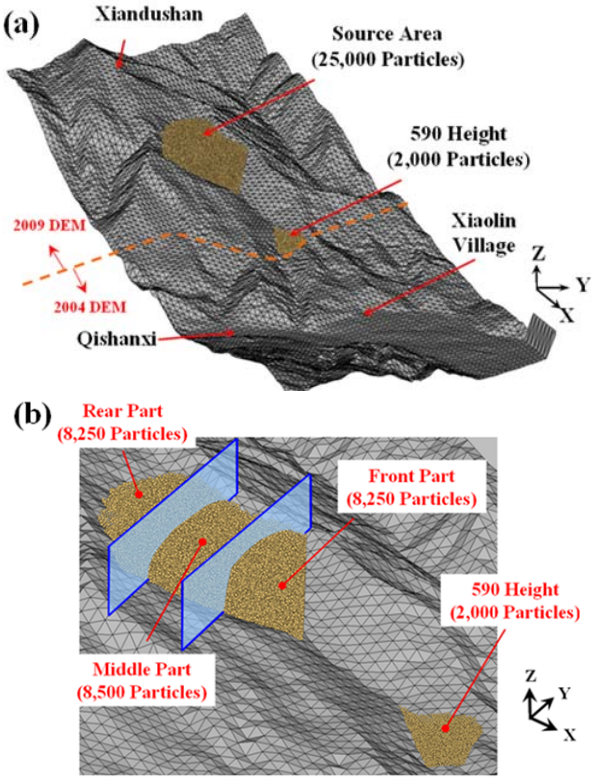

Figure 5 The Hsiaolin landslide modeling. (a) the sliding surface of the collapse area was constructed by 13,456 wall elements based on DEM data (after Morakot event), and the deposit area was used DEM data (before the Morakot event); and (b) diagrams the location of velocity measurement parts.

In this paper, the sliding mass of the Hsiaolin landslide model initially glued (bonded) together on source area which used the strength of Yenshuikeng Shale at each bonding zones; then, the 590 Height did not used the bonding model on each particles which reflect the loose debris material properties. Finally, the parameter of viscous damping in PFC3D influences the motion of particles and reflects energy loss during collision. The damping parameters were used the experiment results in the field by Giani (1992) (Tab.3).

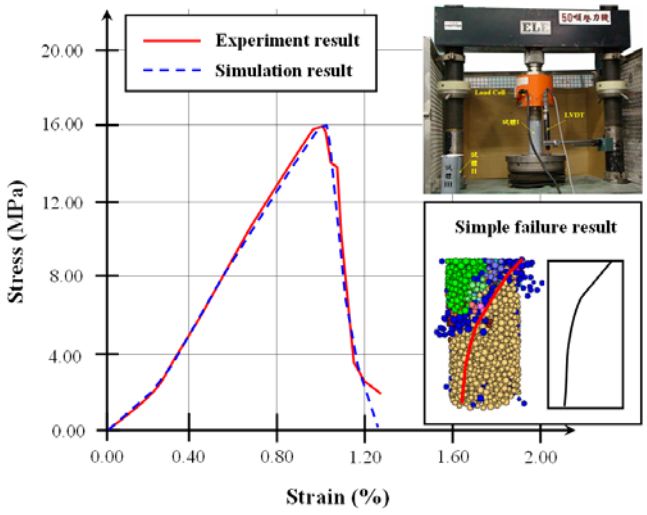

Figure 6 The comparison result of real and simulation uniaxial compression test.

Comparison of simulation results

Fig.7 presents the comparison of simulation results of 5 m resolution DEM with the final deposition pattern. In order to find the best fitting parameters, we chosen 36 ground control points (GCPs, the collapsed area of the landslide dam has been excluded) to compare deposition pattern and calculate the errors for different friction coefficients, bond strengths, and contact stiffness modeling. According to Tab.4 and Fig.7, the simulation thickness distribution closely matches the measured thickness distribution throughout the deposit (DEM data). Best fitting parameters are a friction coefficient for each slip surface equal 0.1, bond strength of 16 MPa, and contact stiffness of 4.8×10^{10}-1×10^{11} kN/m.

Table 4 The comparison result of deposit extent and deposit thickness for different friction coefficients, bond strengths, and contact stiffness modeling.

Numerical modeling		Deposition extent error (m)	Deposition thickness error (m)
Friction coefficients	0.05	18.32	13.57
	0.1	**3.65**	**4.22**
	0.15	43.27	31.60
	0.2	116.21	47.13
Bond strength (MPa)	2	5.25	5.68
	20	**3.43**	**4.35**
	200	52.64	35.55
Contact stiffness (kN/m)	2×10^6	43.25	32.27
	2×10^7	15.44	12.32
	2×10^8	**3.41**	**3.98**
	2×10^9	7.52	8.53

* Deposition thickness error $= \frac{\sum_{1}^{N}(\text{DEM value} - \text{simulation value})}{N}$

*N: number of the comparison value (N=36 GCPs)

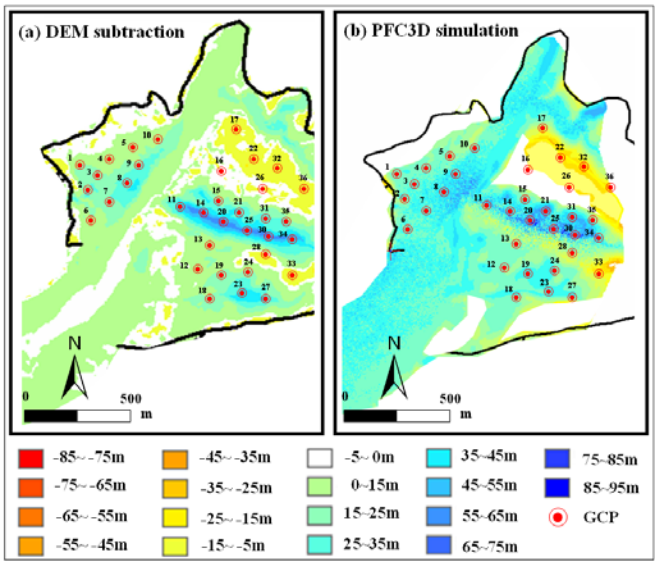

Figure 7 The comparison of simulation results: (a) 5 m resolution DEM subtraction between 2004 and 2009; (b) DEM subtraction by numerical simulation.

Simulation Results of Kinematics model

In order to interpret the kinematic process of Hsiaolin landslide, the main slide mass was divided into three parts: the front, the middle, and the rear. They contained ball elements of 8,250, 8,500, and 8,250, respectively (Fig.6). Velocity measurements along X, Y, Z direction were conducted to interpret the interaction and the kinematic process (Fig.8). The simulation results of kinematic process are explained as follows:

a. Fig.9 and Fig.10 diagram the velocity for each particle. The maximum velocity was about 70 m/s occurred within 10-15 s while the landslide was in a downward plunging motion towards the top of High-Level Terrace from the source area. The velocity was about 32-50 m/s on High-Level Terrace; at 30-65 s, most of the particles slipped into Unnamed Creek A and the velocity was about 30-62 m/s, some particles slipped into Unnamed Creek B with velocity at about 45-68 m/s. When the debris avalanche reached and destroyed the Hsiaolin village, the velocity was about 35-60 m/s within 50 s. Most of the remaining particles were strewn along Unnamed Creek A and ran-up on the right bank of the Qishanxi stream in 60-70 s, the velocity was about 25-30 m/s (Fig.9). The velocities for different time intervals for each part of the slide are depicted in Fig.9. This result revealed that significant influence for strength loss and collision interaction of Hsiaolin landslide.

b. In X direction, the maximum velocity for each cluster occurred within 15 s (about 64 m/s, in front part), 30 s (about 64 m/s, in middle part), 39 s (about 55 m/s, in rear part), and 19 sec (about 44 m/s, in 590 Height), respectively (Fig.10a-10d). In these stages, every part of the main slide mass was capable of reaching the top of the High-Level Terrace from the source area. Material fragmentation and collapse of colluvial deposits into debris commenced within 2 s in front part, 5 s in middle part, and 9 s in rear part, respectively. This reflected the loss of strength of the disintegrated rock mass and the materials were about to transform into a debris avalanche. The front part hit 590 Height approximately within 15 s after the landslide was initiated. The 590 Height commenced to shift. 590 Height eventually collapsed and the loosened colluvial materials were integrated into the debris materials, and were spread out on High-Level Terrace. This interaction subsequently caused deceleration in the front part (Fig.10c and Fig.10d). Within 50-75 s the velocity of the entire debris mass, including materials from 590 Height, suddenly accelerated again. The debris avalanche overflowed the top of High-Level Terrace, and then passed through the end of the High-Level Terrace to reach Hsiaolin village and beyond. Most of the slide mass slipped and spilt into Unnamed Creek A gradually decelerated, and then the collision interaction for each particle caused the front part to run-up to the right bank of the Qishanxi stream. The amplitude of velocity for each particle indicated a degree of the collision interaction in landslide process. The measured results of X direction velocity showed a significant collision interaction time for 16-65 s in front part, 32-80 s in middle part, 39-105 s in the rear part, and 15-75 s in 590 Height, respectively. This reflected that most of the collision interactions controlled the landslide motion at these steps. Movement processes from High-Level Terrace to Unnamed Creek A to the Qishanxi stream were related to the collision interaction for each cluster in sequence. All of the particles stopped motion (velocity equaled 0) and formed the landslide dam at about 112 sec.

c. In Y direction, the negative velocity denotes slide mass motion toward the south; the positive velocity denotes that slide mass motion toward the north. The maximum positive velocity of each cluster occurred within 26 s, with velocity around 20 m/s, in front part; 35 s (about 22 m/s, in middle part), 44 s (about 21 m/s, in rear part), and 27 s (about 17 m/s, in 590 Height), respectively (Fig.10e-10h). In these stages, the front part had caused collapse of 590 Height, thus allowed debris avalanche overflow and spread onto the High-Level Terrace, most of the collision interaction controlled the landslide motion at this step. Observation of negative velocity showed that the maximum negative velocity of some particles occurred in 18 sec (about 42 m/s, in front part), 33 s (about 42 m/s, in middle part), 44 s (about 21 m/s, in rear part), and 42 s (about 49 m/s, in 590 height), respectively, illustrating that some of the slide mass slipped into Unnamed Creek B and attained very high velocity through steeply inclined terrain.

d. In Z direction, the negative velocity denotes downward motion (free fall or downward slide behavior) of the slide mass; the positive velocity denotes upward motion (bounce or run-up motion behavior) of the slide mass. Most of the velocities showing negative value in each cluster were indicative of the steep terrain and high potential energy that caused a significant downward motion of Hsiaolin landslide (Fig.10i-10l). The positive velocity for each part occurred, respectively, at 16-67 s (about 5-20 m/s, in front part), 20-53 s (about 3-18 m/s, in middle part), 32-68 s (about 3-15 m/s, in rear part), and 17-63 s (about 5~19 m/s, in 590 Height). This indicated the significance of collision interaction and terrain variation that caused parts of the cluster to have bounce or run-up motions on High-Level Terrace at this step. The front part travelled freely without obstruction until it hit 590 Height, hence the cluster of front part was accelerating; speed of the middle part was decreasing slightly, while the rear part was smaller and much slower than the others. The same situation occurred within 16 s; the negative velocity of the front part decreased slightly and accelerated the cluster of 590 Height.

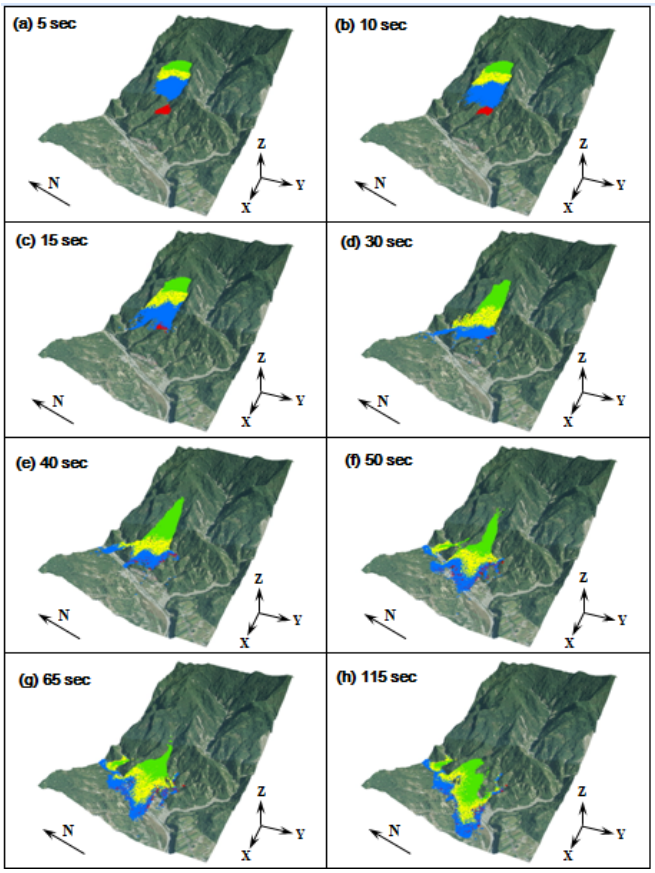

Figure 8 Diagrams kinematic process of the Hsiaolin catastrophic landslide. Blue color is the front part of the landslide mass, yellow color is the middle part, green color is the rear part, and red color is 590 Height.

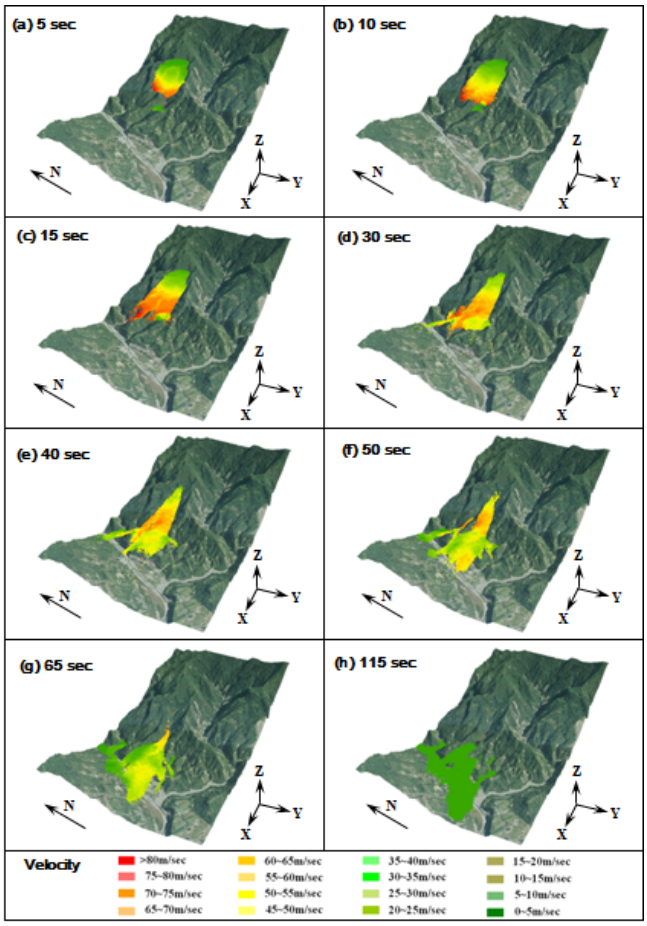

Figure 9 Diagrams the velocity and kinematic process of the Hsiaolin landslide.

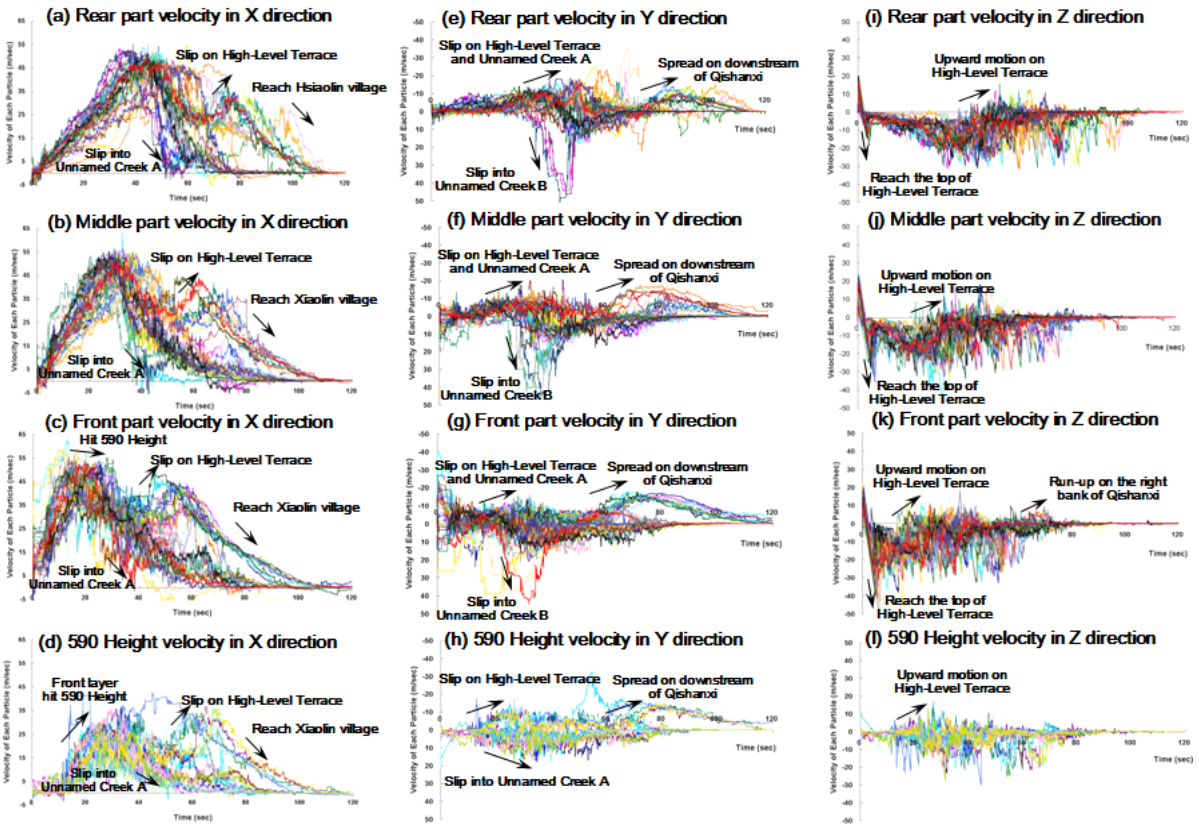

Figure 10 The results of the velocity measurements in X, Y, Z directions; different color lines diagrams the velocity of landslide process for each particle.

Conclusion

In this article, the geomorphologic analysis revealed that the source area was covered by very thick colluvium originated during the period 1936-2009. In 1936, the colluvium constructed 590 Height within the top of High-Level Terrace. The river course was consequently deflected and provided the evidence of past landslide activity. Numerical analysis suggested that when the landslide mass reached the gentle slope, the velocity was about 50-70 m/sec; the steep terrain, the gravity, and the collision interactions controlled the landslide motion. At 20-65 s, 590 Height collapsed when attacked by Hsiaolin landslide. The hummocky terrain was thus transformed into the smooth terrain, which in turn provided debris avalanche that overflowed High-Level Terrace. In this stage, the velocity was about 32-50 m/s, most of the collision interaction and fluidization controlled the landslide motion at this step. Hsiaolin village was destroyed at 60-65 s. All of the particles stopped motion and formed the landslide dam after 112 sec.

This study reflects that the discrete element method, which is not a main stream computational tool, has great potential for gaining mechanical understanding, and also for hazard delineation. A kinematic model of landslide through the discrete element method is developed, which enables a fundamental assessment of landslide mechanism, debris mass motion, deposition extent, and the severity of damage caused by the landslide.

References

Cundall P A, Strack OD (1979) A discrete numerical model for granular assemblies. Geotechnique 29: 47-65.

Dong J J, Li Y S, Kuo C Y, Sung R T, Li M H, Lee C T, Chen C C, Lee W R (2011) The formation and breach of a short-lived landslide dam at Hsiaolin village, Taiwan - Part I: Post-event reconstruction of dam geometry. Engineering Geology, doi: 10.1016/j.enggeo.2011.04.001.

Giani G P (1992) Rock slope stability analysis. A. A. Balkema, Rotterdam, 361.

Hungr O (2007) Dynamics of rapid landslides. Progress in Landslide Science, Chapter 4: 47-56.

Lee C T, Dong J J, Lin M L (2009) Geological investigation on the catastrophic landslide in Siaolin village, southern Taiwan. Sino-Geotechnics 122: 87-94.

Potyondy D O, Cundall P A (2004) A bonded-particle model for rock. International Journal of Rock Mechanics & Mining Sciences 41: 1239-1364.

Steven N W, Simon D (2006) Particulate kinematic simulations of debris avalanches: interpretation of deposits and landslide seismic signals of Mount Saint Helens, 1980 May 18. International Journal of geophysics 167: 991-1004.

Sung Q C, Lin C W, Lin W H, Lin W C (2000) Chiahsien. Explanatory text of the geological map of Taiwan 51: 33-37.